Journal of BUON **9**: 83-89, 2004
© 2004 *Zerbinis Medical Publications. Printed in Greece*

ORIGINAL ARTICLE

The effect of asymmetric collimation on the dose distribution and verification of treatment planning system for asymmetric fields

B. Demir[1], H. Bilge[2], B. Günhan[1], A. Koca[1], S. Karaçam[1]

[1]Department of Radiation Oncology, Cerrahpaşa Medical Faculty, University of Istanbul, Istanbul; [2]Department of Medical Physics, Oncology Institute, University of Istanbul, Istanbul, Turkey

Summary

Purpose: *This study reports the feasibility of the symmetric fields for the usage of asymmetric fields, and checks the accuracy of treatment planning system (TPS).*

Materials and methods: *A GE Saturne-42 linear accelerator, which produces dual photon energies of 6 and 15 MV, and an ISIS-3D TPS were used in this study. Percent depth doses (PDDs), dose profiles, and isodose distributions for symmetric and asymmetric fields were generated in a water phantom and these data were compared to those calculated by the TPS.*

Results: *When the results were compared it was seen that the PDDs decreased with increasing off-axis distance and depth. The PDDs comparison demonstrated that for 15 MV, asymmetric and symmetric field PDDs can differ by as much as 4%, and the differences between the calculated by the TPS and the measured PDDs for asymmetric fields were less than 2%. It was also seen that the penumbra of symmetric and asymmetric fields were very close to each other and the difference between the calculated and the measured ones were less than 2 mm. The comparison between the measured and calculated isodose distributions for 6 and 15 MV photon beams for asymmetric field showed that a good agreement has been achieved in general, and the differences between the field edges and near the centre of the fields were found within 2 mm.*

Conclusion: *This study shows that the measured and calculated data using water phantom and TPS (ISIS-3D), respectively, were in good agreement. Therefore TPS can be used safely for asymmetric fields in routine practice.*

Key words: asymmetric collimator, isodose, linear accelerator, penumbra, percent depth dose, treatment planning system

Introduction

Asymmetric collimators are now available on all modern linear accelerators. These are collimators that allow for the independent movements of each of the four field- defining jaws. Asymmetric collimation can be used as a replacement for cerroband blocks when the block has an edge that is parallel to the treatment field. The use of a half-collimated asymmetric field (i) in joining two adjacent fields, (ii) in avoiding the beam divergent problem near critical structures and (iii) in tangential opposed breast, parallel opposed head-neck techniques, will simplify set-up and improve dose distribution [1-5]. The full potential of asymmetric collimation can be realized only with proper dose calculation algorithms. Treatment plans can then be optimised with asymmetric fields. Chui et al. [6] have extended a method, originally developed for symmetric fields, to calculate dose distributions for asymmetric fields. In this method, measured central axis depth doses and beam profiles for symmetric fields are employed. Presently, treatment planning algorithms that compute dose distributions in asymmetric fields are based on symmetric fields data. Before starting to use TPS they had to be checked with the measured data and the differences had to be within acceptable limits. There is not any comparison of the measured values and the taken

Received 12-10-2003; Accepted 25-11-2003

Author and address for correspondence:

Bayram Demir, M.Sc
University of Istanbul
Cerrahpaşa Medical Faculty
Department of Radiation Oncology
A.B.D. 34303
Fatih
Istanbul
Turkey
Tel: +90 212 414 30 00 / 21187
Fax:+90 212 414 30 97
E-mail: baybay@istanbul.edu.tr

values from ISIS-3D (Technologie Diffusion) for asymmetric fields in the literature.

This study reports the feasibility of the symmetric fields for the usage of asymmetric fields and checks the accuracy of TPS (ISIS-3D) which has been used in our department (Department of Radiation Oncology, I.U. Cerrahpaşa Medical Faculty).

Materials and methods

Equipment

Linear accelerator

The Saturne-42 linear accelerator, which was used in our study, produces 6 and 15 MV photon energies as well as eight electron energies ranging between 4.5 and 21 MeV. At 100 cm Source-Axis-Distance (SAD) the field size can be opened from 4×4 cm^2 to 40×40 cm^2, and for electron energies the field size can be opened from 2×2 cm^2 to 30×30 cm^2 with trimmers. The asymmetric collimation is provided with the lower jaws X_1 and X_2. X_1 and X_2 jaws cannot pass the central axis and in the photon case the range is 0-200 mm, whereas for electrons it is 0-150 mm. Y_1 and Y_2 are unable to move asymmetrically. The geometry of one-dimensional asymmetric collimators is shown in Figure 1.

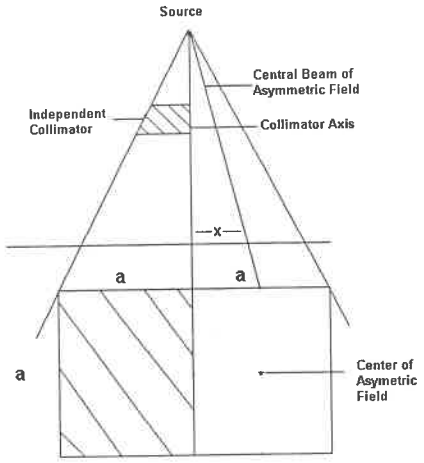


Figure 1. Geometry of an axa cm^2 asymmetric field, generated from a 2axa cm^2 symmetric field.

x=the distance between the collimator axis and the centre of the asymmetric field

Treatment planning system

The calculation method of the ISIS-3D for the asymmetric field uses the same set of data created previously for symmetric fields, like PDDs, open field profiles, open field profiles along the diagonal of the largest field size (40×40 cm^2), and scatter variation curves. The algorithm that is used by ISIS-3D for the calculation of dose in one point is based on the separation of primary and scatter radiation. This has been proposed by Johns and Cunningham [7], based on the original idea developed by Clarkson [8]. The dose D (x, y, z) at a point P of coordinates x, y, z, at a depth p is calculated by integrating over circular sectors as follows:

$$D(p,r) = P(p) + \sum \Delta S(p,r_i)$$

where:

$\Delta S(p,r_i)$ is the scattering from an angular sector of radius r_i.

The contribution of primary radiation

The contribution of primary radiation to the dose at a point P can be written as:

$$P(x,y,z) = TAR(p,o) \times I \times C(x,y) \times W(x,y)$$

where:

TAR (p,o) is the Tissue – Air Ratio at a depth p for a field of zero section (primary transmission); I is the correction factor that accounts for the inverse square (of the distance to the source) law; C (x,y) is the correction factor that accounts for the point position relative to the opening defined by the collimator and the blocks; and W (x,y) is a correction factor that accounts for the presence of wedge filters.

The contribution of scatter radiation

The scatter contribution to the dose at a point P is the sum of the elementary scatter $\Delta S_i(p,r_i)$ corresponding to the contribution at a depth p at a point x, y with an elementary scatter volume ΔV_i exposed to the primary radiation P_i.

The scatter is: $(\alpha_i / 360) \times SAR(p,r_i)$ where:

$SAR(p,r_i)$ is the scatter air ratio at a depth p for a circular field of radius r_i; r_i and α_i are the radius and the angle, respectively, of the considered sector.

The $SAR(p,r_i)$ are calculated by interpolation starting with the tables 'primary-scatter' saved in the machine's library for 20 depth and 20 radius' values.

The SAR values from the tables are obtained from experimental data using the equation:

$$SAR(p,r) = TAR(p,r) - TAR(p,0).$$

A detailed description of the algorithm for the calculation of dose in one point can be found in the creation of the treatment unit library of ISIS-3D [9].

Measurement

Percent depth dose

In this study, the PDDs of symmetric and asymmetric fields were measured at 100 cm Source-Skin

Distance (SSD) between 0-20 cm depth at the central beam of the symmetric and asymmetric field using a water scanning equipment for 5×5 cm², 10×10 cm² and 20×20 cm² field sizes and off-sets up to 2.5, 5, 7,5 and 10 cm. The Wellhöfer scanning system consists of the water phantom interfaced to a personal computer. Two 0.14 cc IC10 type chambers were used this water scanning system. The depth dose curves were normalized to the depth of dose maximum. For the same field sizes, depths, and off-axis distances, the PDDs were calculated by TPS, and then the PDDs, which were calculated by the TPS and those measured with the water phantom at selected depths, were tabulated for comparison (Table 1).

Table 1. The PDDs of measured and those obtained from the TPS for symmetric and asymmetric fields for 6 and 15 MV

	0 cm off-axis			*2.5 cm off-axis*			*5 cm off-axis*			*7.5 cm off-axis*			*10 cm off-axis*		
Depth cm	Measured	TPS	Difference %	Measured	TPS	Difference %	Measured	TPS	Difference %	Measured	TPS	Difference %	Measured	TPS	Difference %
						6 MV									
	Collimator setting (–2.5, 2.5)×5 cm²			(0, 5)×5 cm²											
5	86.30	86.66	0.4	86.10	86.66	0.6									
10	65.40	65.45	0.1	65.30	65.48	0.3									
20	37.30	37.44	0.4	37.10	37.38	0.7									
	(–5, 5)×10 cm²			(–2.5, 7.5)×10 cm²			(0, 10)×10 cm²								
5	87.50	87.50	0.0	87.50	87.50	0.0	87.50	87.50	0.0						
10	68.50	68.59	0.1	68.30	68.27	0.0	68.30	68.15	0.2						
20	40.50	40.73	0.6	40.40	40.55	0.4	40.30	40.40	0.2						
	(–10, 10)×20 cm²			(–7.5, 12.5)×20 cm²			(–5, 15)×20 cm²			(–2.5, 17.5)×20 cm²			(0, 20)×20 cm²		
5	88.20	88.33	0.1	88.00	88.33	0.4	88.00	87.92	0.1	87.90	87.92	0.0	87.90	87.50	0.5
10	70.90	71.00	0.1	70.60	70.27	0.5	70.70	70.03	1.0	70.30	70.08	0.3	70.30	70.21	0.1
20	44.20	44.21	0.0	44.20	43.78	1.0	43.80	43.55	0.6	43.50	43.51	0.0	43.10	43.48	0.9
						15 MV									
	(–2.5, 2.5)×5 cm²			(0, 5)×5 cm²											
5	95.30	95.10	0.2	95.00	94.70	0.3									
10	76.80	76.62	0.2	76.40	76.36	0.1									
20	49.30	48.54	1.6	49.10	48.37	1.5									
	(–5, 5)×10 cm²			(–2.5, 7.5)×10 cm²			(0, 10)×10 cm²								
5	94.80	95.27	0.5	94.90	95.08	0.2	94.40	94.79	0.4						
10	77.70	78.07	0.5	77.80	77.71	0.1	77.30	77.42	0.2						
20	51.40	51.43	0.1	51.30	51.22	0.2	50.70	50.87	0.3						
	(–10, 10)×20 cm²			(–7.5, 12.5)×20 cm²			(–5, 15)×20 cm²			(–2.5, 17.5)×20 cm²			(0, 20)×20 cm²		
5	94.20	94.40	0.2	94.10	94.21	0.1	93.30	93.93	0.7	93.00	93.74	0.8	92.80	93.55	0.8
10	78.10	78.47	0.5	77.90	78.00	0.1	77.40	77.78	0.5	76.70	77.61	1.2	76.30	77.58	1.6
20	53.20	52.98	0.4	53.00	52.70	0.6	52.30	52.44	0.3	51.50	52.36	1.6	51.10	52.00	1.7

Table 2. The penumbra values generated from the TPS and those measured for symmetric and asymmetric fields for 6 and 15 MV

6 MV										
		Depth: 1.6 cm			*Depth: 5 cm*			*Depth: 10 cm*		
Field size cm²	*Off-axis Distance cm*	*Measured Penumbra (80-20)%*	*TPS Penumbra (80-20)%*	*Difference mm*	*Measured Penumbra (80-20)%*	*TPS Penumbra (80-20)%*	*Difference mm*	*Measured Penumbra (80-20)%*	*TPS Penumbra (80-20)%*	*Difference mm*
5×5	0	7.0	7.9	0.9	6.6	7.9	1.3	7.9	8.3	0.4
	2.5	7.2	7.7	0.5	6.5	7.8	1.3	7.9	8.1	0.2
10×10	0	7.2	8.0	0.8	7.2	8.3	1.1	9.2	9.2	0.0
	2.5	7.0	8.1	1.1	7.3	8.2	0.9	8.9	8.7	0.2
	5	7.0	7.9	0.9	7.1	8.3	1.2	8.9	8.9	0.0
20×20	0	8.4	8.1	0.3	9.1	8.2	0.9	10.6	9.6	1.0
	2.5	8.2	8.1	0.1	9.3	8.5	0.8	10.5	9.2	1.3
	5	8.3	8.2	0.1	9.4	8.5	0.9	10.4	9.9	0.5
	7.5	8.3	8.3	0.0	9.0	8.7	0.3	10.3	9.4	0.9
	10	8.2	8.5	0.3	9.2	9.0	0.2	10.3	10.2	0.1
15 MV										
		Depth: 3 cm			*Depth: 5 cm*			*Depth:10 cm*		
5×5	0	7.2	7.9	0.7	7.6	7.6	0.3	8.4	8.3	0.1
	2.5	8.1	7.6	0.5	7.3	7.3	0.4	7.9	7.9	0.0
10×10	0	8.8	8.0	0.8	8.1	8.1	0.2	9.0	8.8	0.2
	2.5	8.0	8.0	0.0	8.1	8.1	0.1	8.7	8.5	0.2
	5	7.7	7.9	0.2	8.1	8.1	0.1	8.8	8.5	0.3
20×20	0	9.3	8.5	0.8	8.8	8.8	0.4	9.9	9.1	0.8
	2.5	8.4	8.4	0.0	8.8	8.8	0.4	10.7	8.9	1.8
	5	8.5	8.6	0.1	9.9	9.9	1.5	10.3	9.1	1.2
	7.5	9.7	8.7	1.0	10.0	10.0	1.3	10.8	9.1	1.7
	10	9.9	8.5	1.4	9.3	9.3	0.8	10.0	9.1	0.9

Penumbra (profile)

Beam profiles along the central axis of the fields were measured at depths of dose maximum (1.6 mm for 6 MV and 3 mm for 15 MV), 5 and 10 cm for 5×5, 10×10, and 20×20 cm² field size at the same off-axis distance with the PDDs measurement. The beam profiles were normalized to PDDs of the measured depth at the central beam of the symmetric and asymmetric field. The penumbra was defined as the distance between the 80% and 20% dose line near the edge of the field for a reference depth. Dose profiles for the same field sizes, depths and off-axis distances were calculated by TPS to obtain the penumbras (Table 2). As an example of the dose profiles from which Table 2 was generated, Figure 2 compares dose profiles measured for 10×10 cm² half-collimated asymmetric field with 5 cm off-axis (with one jaw closed down to the collimator central axis from a 20×10 cm² symmetric field) and calculated by TPS for the same conditions.

Isodose

Isodoses measurement for 6 and 15 MV photon beams were performed for field sizes of 5×5, 10×10, and 20×20 cm² symmetric and half-collimated asymmetric fields at 100 cm SSD between 0-20 cm depth with water phantom, and the isodoses were normalized to the depth of dose maximum. To study the ef-

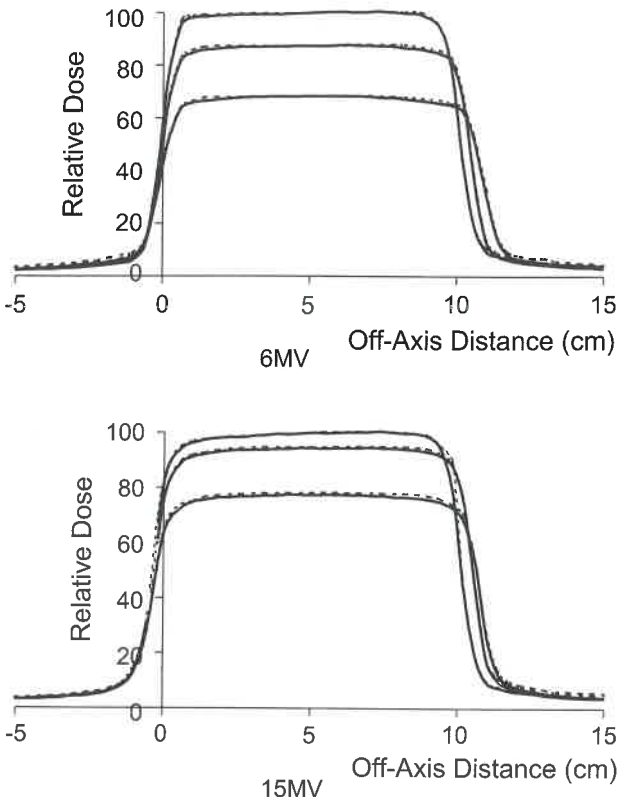


Figure 2. Dose profiles at dose maximum (1.6 mm for 6 MV and 3 mm for 15 MV), 5, 10 cm depth for 10×10 cm² field size with 5 cm off-axis distance from water phantom (solid line) and TPS (broken line).

fect of asymmetric collimation on the isodose distributions, symmetric and asymmetric fields of the same field sizes were superimposed. As an example of the isodose distributions, Figure 3 compares the isodose

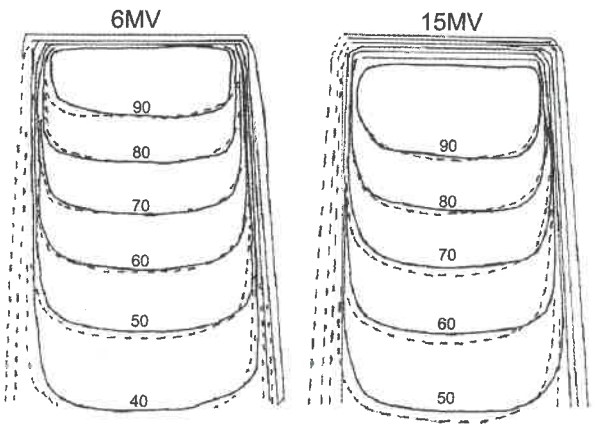


Figure 3. Measured isodoses using water phantom for 10×10 cm² symmetric field (broken line) and 10×10 cm² asymmetric field with 5 cm off-axis distance (with one jaw closed down to the collimator central axis from a 20×10 cm² symmetric field) (solid line).

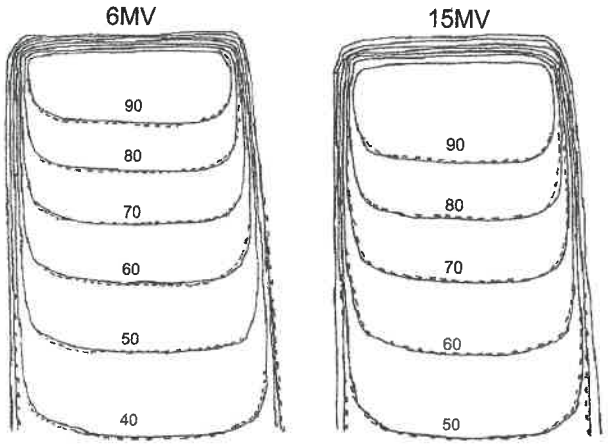


Figure 4. Isodose distributions for 10×10 cm² field size with 5 cm off-axis distance from water phantom (broken line) and TPS (solid line).

distribution of a 10×10 cm² field size for symmetric and asymmetric field settings.

The isodose distributions were generated by the TPS for the same conditions. Figure 4 shows the superimposition of the isodose distributions scanned with the water phantom and generated by the TPS for 10×10 cm² half-collimated asymmetric field with 5 cm off-axis.

Results

Percent depth dose

In our study for both energies, as the off-axis distances and depth were increased, the PDDs of the asymmetric fields decreased relative to PDDs of the symmetric fields. The decrease in PDDs for 6 and 15 MV could be as high as 2.5% and 4.0%, respectively (Table 1).

When the results in Table 1 were compared, the largest deviation in the PDDs between the measured and calculated ones for 20×20 cm² field size was 1% and 1.7% for 6 MV and 15 MV, respectively (Table 1). The PDDs obtained from the water phantom and the TPS for symmetric and asymmetric fields were in accordance with each other and were fulfilling the requirements of ICRU [10].

Penumbra

The results of penumbra measurement at 5×5, 10×10, and 20×20 cm² for 6 MV and 15 MV are shown in Table 2. At both energies there was not a significant variation in the penumbra of the symmet-

ric and asymmetric fields depending on the off-axis distances. The largest difference between the penumbra values of the symmetric and asymmetric fields was 1.2 mm. This was observed at 15 MV for 20×20 cm^2 symmetric field and also at 5 cm depth of 20×20 cm^2 asymmetric field with 7.5 cm off-axis distance.

When we compared the measured and the calculated penumbras, it was seen that the values were in good agreement with each other and the difference was 1.3 mm for 6 MV and 1.8 mm for 15 MV. The difference between the measured and calculated penumbras for all fields and depths shown on Table 2 were within the acceptance criteria of 2 mm of ICRU [10].

Isodose

In Figure 3, where the comparison of isodose distribution of symmetric and asymmetric fields are given, it is shown that, the divergence on the asymmetry applied side of the field is decreased with depth, whereas on the other side it is increased. It was also seen that, depending on the flattening filter structure, there had been differences between the isodose distribution of symmetric and asymmetric fields and the difference went up to 7-8 mm for 15 MV on both sides of the central axis of the fields.

The comparison of measured and calculated asymmetric fields isodose distributions for 6 and 15 MV photons beams showed that there was a good agreement between the measured and calculated data. The deviations near the centre of the fields were smaller than 2 mm, which is the limit of acceptance recommended by ICRU [10]. The deviation in the field edges was within 2 mm.

Discussion

To increase the local cancer control rate by radiotherapy and to reduce the damage to the surrounding healthy tissues, the latest technology has to be used. All these efforts are made to achieve a treatment free of error. This is so-called "Conformal Therapy". The first step of this improvement is the implementation of the asymmetric jaws setting to the linear accelerators, which is used in the treatment of adjacent radiation fields.

In the linear accelerators, when accelerated electrons hit the target, which is made of high atomic number elements, high energy X-rays (bremms rays) are produced. X-rays produced via low energy electrons have more side scatter, whereas X-rays produced via high energy electrons have increased forward scatter. Therefore X-ray beams have the shape of a water drop; that is why they cannot be used in the treatment. To flatten the shape of the beam in the depth of treatment, a beam-flattening filter is put in front of the beam. Generally, the design of the flattening filter imitates the shape of a drop [11]. Nevertheless, when one uses the flattening filter in the asymmetric case will obtain different parameters from the symmetric case. The effect of asymmetric collimation to dose distribution was first shown by Loshek [12]. In this study collimator scattering and deviation in off-axis beam profiles were investigated. These deviations, which came out as a result of the asymmetric usage of the beam flattening filter, were the characteristics of the flattening filter and might differ from filter to filter in dosimetric parameters like symmetric fields PDDs and profiles and isodoses.

In the first part of the study, it was observed that the difference in the PDD could be over 2%, but, on the other hand, the differences in the penumbra values were under 2 mm. The difference between the isodose distribution of symmetric and asymmetric fields was found over 2 mm. As it was expected, the beam divergence on the asymmetry applied side of the field was eliminated.

In the second part of the study, we concentrated on the TPS, which has a very important role in dose optimisation. The most important future of the modern TPS is to do 3D dose calculations with the least dosimetric data. Nevertheless, the accuracy of the dose calculation algorithm of the TPS has to be investigated. In particular, asymmetric field dose calculation is directly dependent on the accuracy of the TPS. This accuracy of the TPS is affected from the experimental determination of the primer and scatter component of the dose, as well as the algorithm of the TPS.

In this study, we measured the PDDs, penumbras and the isodose distributions of 6 and 15 MV photon beams produced from a Saturne-42 linear accelerator in our clinic and we tested these experimental data with those generated from the TPS. Looking into the data generated from the TPS and those generated from the water phantom, we assume that the measured and the calculated data were in good agreement and the observed differences, were within the limits recommended by ICRU [10].

References

1. Dittmer PH, Randal ME. A technique for inguinal node boost using photon fields defined by asymmetric collimator jaws. Radiother Oncol 2001; 59: 61-64.

2. Klein EE, Taylor M, Michaletz-Lorenz M, Zoeller D, Umfleet W. A mono isocentric technique for breast and regional nodal therapy using dual asymmetric jaws. Int J Radiat Oncol Biol Phys 1994; 28: 753-760.
3. Kwa W, Tsang V, Farirey R. Clinical use of asymmetric collimator. Int J Radiat Oncol Biol Phys 1997; 37: 705-710.
4. Özyar E, Işın G, Uzal D, Güldallı S, Arslan G. Asymmetric collimation and its clinical application. Türk Onkoloji Dergisi 1995; 10: 48-52.
5. Sohn WJ, Suh HJ, Pohar S. A method for delivering accurate and uniform radiation dosages to the head and neck with asymmetric collimators and a single isocenter. Int J Radiat Oncol Biol Phys 1995; 32: 809-813.
6. Chui CS, Mohan R, Fontenla D. Dose computations for asymmetric fields defined by independent jaws. Med Phys 1988; 15: 92-95.
7. Johns HE, Cunningham JR (eds). Calculation of dose at any point. In: The Physics of Radiology (4th edn). CC Thomas, Springfield, Illinois, 1983, pp 369-380.
8. Steidley KD, Gamper C, Greener A, Caggiano A. A Clarkson's sector integration routine for personal computers. Med Phys 1994; 21: 61-64.
9. Boisserie G, Drouard J, Rosenwald JC, Zelkifi S. Creation of the treatment unit library for iSis2, iSis3D, Calcum, Plex programs. May 1998.
10. International Commission on Radiation Units and Measurements. Use of computers in external beam radiotherapy procedures with high energy photon and electron. ICRU Report No 42, Bethesda, USA, 1987.
11. Ahnesjö A. Analytic modelling of photon scatter from flattening filters in photon therapy beams. Med Phys 1994; 21: 1227-1235.
12. Loshek DD. Applications and physics of the independent collimators feature of the Varian Clinac 2500. Proc 10th Varian Users Meeting, April 15-17 1984, Palm Spring, California, pp 81-87.